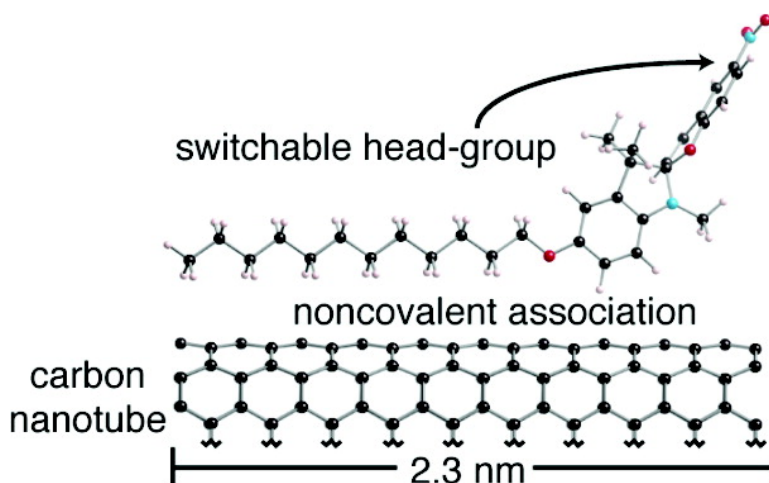


Directing and Sensing Changes in Molecular Conformation on Individual Carbon Nanotube Field Effect Transistors

Xuefeng Guo, Limin Huang, Stephen O'Brien, Philip Kim, and Colin Nuckolls

J. Am. Chem. Soc., **2005**, 127 (43), 15045-15047 • DOI: 10.1021/ja054335y • Publication Date (Web): 07 October 2005

Downloaded from <http://pubs.acs.org> on March 25, 2009



More About This Article

Additional resources and features associated with this article are available within the HTML version:

- Supporting Information
- Links to the 11 articles that cite this article, as of the time of this article download
- Access to high resolution figures
- Links to articles and content related to this article
- Copyright permission to reproduce figures and/or text from this article

[View the Full Text HTML](#)

Directing and Sensing Changes in Molecular Conformation on Individual Carbon Nanotube Field Effect Transistors

Xuefeng Guo, Limin Huang, Stephen O'Brien, Philip Kim,* and Colin Nuckolls*

The Nanoscience Center and Departments of Chemistry, Applied Physics/Mathematics, and Physics, Columbia University, New York, New York 10027

Received June 30, 2005; E-mail: cn37@columbia.edu

Understanding, directing, and sensing changes in molecular conformation in small collections of molecules is a prerequisite for any nanoscience built around self-assembly. Here we detail a method to detect the assembly of $\sim 10^4$ molecules tagged with photochromic headgroups on an individual carbon nanotube. The important result is that single-walled carbon nanotube field effect transistors (CNTFET)^{1,2} are able to sense the changes in conformation when the molecules are switched. These studies utilize the inherent sensitivity of the CNTFET that arises from their active channel being at the surface and therefore exposed to the environment. The electrostatic and photosensitivity of the CNTFETs forms the basis for a number of sensors^{2,3} and optoelectronic devices⁴ based on carbon nanotube transistors. The unique feature explored here is how to populate the surface of the carbon nanotubes with functional molecules that can be toggled back-and-forth between different molecular conformations (Figure 1A,B).

For this study, we employed the well-known photochromic molecules—spiropyrans—that switch between a neutral, colorless form and a zwitterionic, colored form. The open (merocyanine) form is produced from irradiation with ultraviolet light, while the reverse, spiropyran closure is effected with visible light, as shown in Figure 1B. This photoswitch has been employed in many studies due to the large difference in wavelength of absorbance between the two states and the charge separation in the open form.^{5,6} Particularly relevant to our design are the studies of Haddon and co-workers which show that spiropyrans when covalently attached can alter the optical properties of single-walled carbon nanotubes.⁷ We synthesized^{8,9} versions of the spiropyrans that were derivatized with either alkane or pyrene groups because these moieties have been shown by Dai and co-workers² to noncovalently associate with the surface of carbon nanotubes. In this study, they act as anchors to hold the photoswitchable spiropyrans of **1a** or **2a** in proximity to the tube surface.

To detect the photoswitching effect electrically, we fabricated FETs using isolated semiconducting single-walled carbon nanotubes (SWCNTs) and then functionalized them by self-assembly of **1a** and **2a** from solution.⁸ Individual SWCNTs of high electrical quality were grown by a chemical vapor deposition (CVD) process from CoMo-doped mesoporous SiO₂ catalyst particles using ethanol as the carbon source.¹⁰ The catalyst particles were patterned on doped silicon wafers that had 300 nm of thermally grown SiO₂ on their surface.¹⁰ Source and drain electrodes (5 nm of Cr followed by 50 nm of Au) separated by ~ 20 μm were deposited through a metal shadow mask onto the carbon nanotube samples. Figure 2A shows a representative scanning electron micrograph (SEM) of an individual SWCNT spanning source and drain electrodes on a silicon oxide surface. The doped silicon wafer serves as a global back-gate electrode for the samples.

After initial electrical characterization and selection of individual semiconducting carbon nanotube devices, **1a** or **2a**⁹ were assembled

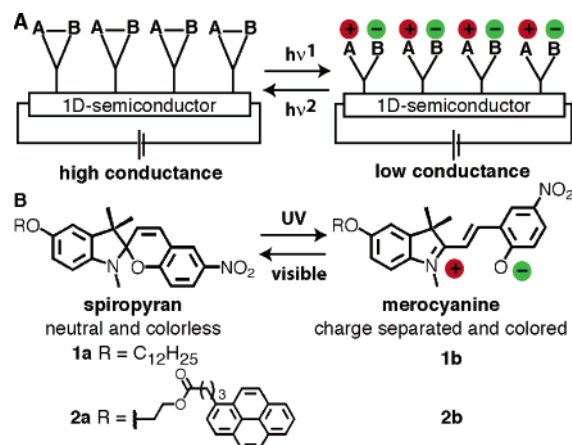


Figure 1. (A) A one-dimensional semiconductor that has molecules assembled on its surface. Light is used to toggle the molecules between a cyclized (left) and charge-separated (right) state. (B) **1a** and **2a** contain a SWCNT recognition domain and a photoswitchable headgroup.

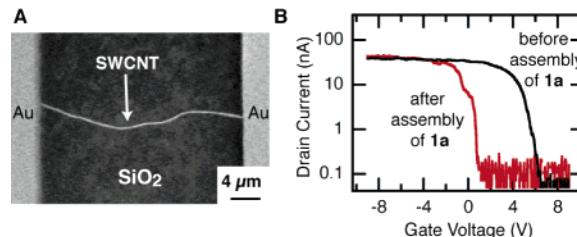


Figure 2. (A) Scanning electron micrograph image of a single carbon nanotube spanning two Au/Cr contacts on a silicon wafer. (B) Semilog plot showing the drain current characteristics of an individual carbon nanotube transistor as a function of gate voltage before and after assembly of **1a** from THF solution. The source drain bias voltage is fixed at 50 mV.

on the surface of the nanotubes by immersion of the devices for 6 h into a THF solution (1.0 mM). The devices were removed from solution and rinsed with acetone and fresh THF. The electrical characteristics of these transistors were noticeably changed after the assembly of **1a** or **2a**. Figure 2B shows the drain current (I_D) as a function of the gate voltage (V_g), while the source-drain bias voltage (V_{sd}) is held at 50 mV before and after assembly of **1a** on the nanotube surface. To eliminate artifacts from gate hysteresis, all of the current voltage curves were acquired on the same measurement cycle while scanning from positive to negative bias. We observe that, for a specific SWCNT device with fixed experimental conditions, very stable $I_D(V_g)$ curves are obtained, and thus they can be used to detect charge transfer and molecular conformation of adsorbed molecules. Initially, a typical p-type semiconductor FET behavior is observed, where I_D raises quickly (on-state) at V_g lower than the threshold voltage, $V_{th} = 5$ V. The on-state resistance (R_{on}) of this FET is ~ 1.2 M Ω . Upon the assembly of the molecules, the device characteristics of the

CNTFET change. While R_{on} remains at a similar level, V_{th} decreases to ~ 1 V. We found this shift in threshold voltage to be universal for CNTFETs with **1a** absorbed on the sidewall of the SWCNT. Since V_{th} decreases as **1a** assembles on SWCNTs, we infer that a net negative charge is being transferred from the assembled molecules to nanotubes.^{11,12}

Mirroring this assembly experiment using the pyrene-tethered spiropyran (**2a**) produces analogous results. The threshold voltage shifts were similar to the dodecane case. [$I_{\text{D}}(V_{\text{g}})$ curves showing this effect are contained in the Supporting Information.] For the **2a**, however, R_{on} becomes larger upon assembly.

We performed three control experiments to test whether the alkane/pyrene anchor, the spiropyran headgroup, or the solvent (THF) is responsible for the V_{th} change. The $I_{\text{D}}(V_{\text{g}})$ curves for these control experiments can be found in the Supporting Information. A first experiment tested the electrical characteristics when devices were immersed in THF, removed, and rinsed with acetone as described above for **1a**. The current–voltage curves show essentially no change in threshold voltage because the solvent is too weak of a binder and cannot survive the washing. A second experiment, which tests the parent spiropyran (1.0×10^{-3} M solutions in THF) for binding, also shows no significant change in V_{th} and R_{on} . The spiropyran lacking the tether is expected to be a poor binder to the nanotube surface because its angular methyl groups encumber π -stacking. The third experiment tests a solution of dodecane or pyrene (1.0×10^{-3} M) in THF. We observe similar shifts in V_{th} to those shown in Figure 2B, implying that the dodecane and pyrene tethers are anchoring to the SWCNT.

Given that the exposed length of the carbon nanotube in these devices is $\sim 20 \mu\text{m}$ long and that **1a** or **2a** would occupy ~ 2 nm of length, on the order of 10 000 molecules would then span the length of these devices. It is unlikely that the origin of this shifting in V_{th} is from charge transfer from the tether molecules, dodecane, or pyrene because these two molecules are chemically and electrostatically very different, yet produce qualitatively similar shifts in threshold. One possibility is that this shift arises from displacement of molecules, such as oxygen, which must coat the tubes in ambient conditions.² The only significant difference between the two tethers is in the on-state resistances of the devices before and after the assembly; while the dodecane produces a negligible change in R_{on} , the pyrene increases it. Although further detailed studies will reveal the mechanism of this observation, these experiments demonstrate that the changes in the transistor characteristics arise from the tethers binding to the surface of the carbon nanotubes, not from the solvent or the spiropyran headgroups.

Once the photochromic molecules are tethered to the surface of the SWCNTs, the device characteristics become very sensitive to light. We found large changes in R_{on} occur in the photochromic CNFET devices when the spiropyran **1a** or **2a** are photoswitched to their charge-separated merocyanine form. Figure 3A shows such a photochromic effect in the **1a**/SWCNT assembly when the device is illuminated by a simple hand-held ultraviolet lamp with a peak wavelength of 365 nm. After ~ 10 min of ultraviolet (UV) irradiation, the initial higher conductance state (red curve, $R_{\text{on}} \sim 0.9 \text{ M}\Omega$) at $V_{\text{g}} \ll V_{\text{th}}$ turns into a lower conductance state (green curve, $R_{\text{on}} \sim 2.5 \text{ M}\Omega$). We note, however, that V_{th} does not change appreciably during this photoswitching process, indicating that the carrier scattering rate is most affected while the carrier concentration and Schottky barrier at the SWNT–electrode junction essentially remain unchanged during the photoswitching of spiropyran. We notice further that the photoswitching effect is a rather gradual process in time. Figure 3B shows a gradual transition from high to low transconductance with current–voltage curves taken every 75 s

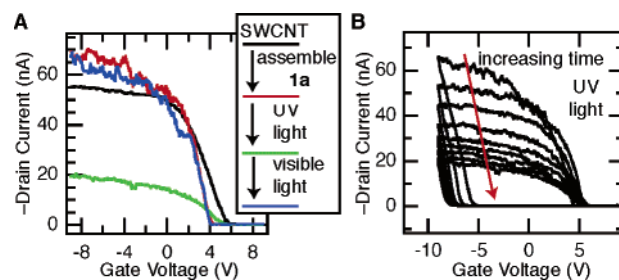


Figure 3. (A) Change in drain current of an individual SWCNT device as a function of V_{g} . The source drain bias voltage is held at 50 mV. Black curve is device before assembly; red curve is device after assembly of **1a**; green curve after irradiation with UV light for ~ 10 min; blue curve after irradiation with visible light. (B) Decrease in drain current of an individual SWCNT device as a function of V_{g} . Data are taken every 75 s as the device is irradiated with UV light. The source drain bias voltage is held at 50 mV.

as the device is irradiated with UV light. R_{on} increases sharply in the beginning of UV illumination and is saturated after ~ 10 min of exposure.

The reverse process in spiropyran (i.e., from charge-separated merocyanine form to the closed spiropyran form) is initiated with visible light.⁶ Figure 3A shows the change of drain current characteristics changes as the UV-photoswitched device is irradiated with visible light (633 nm). After ~ 10 min of exposure to visible light, the device characteristics are essentially restored to the original values before UV irradiation. Devices with **2a** instead of **1a** assembled on their surface can also be switched back-and-forth between high and low conductance states by alternating between UV and visible light, but the magnitude of the effect was lower and the lifetime of these devices was qualitatively shorter.

The reversible switching between high and low conductance states in the functionalized SWCNT FETs suggests that the photoswitching of the tethered molecules is responsible for the change in the transport properties of the semiconducting SWCNT channel. One possibility is that the charge-separated state of the merocyanine introduces scattering sites for the carriers by creating localized dipole fields around the tubes. These sites then scatter charge when it flows in the nearby SWNT channel and thereby lower the mobility in the devices. Another possibility is that the nearby phenoxide ion quenches the p-type carriers in the tubes and behaves like a charge trap. The experiments detailed here do not allow us to distinguish between the two mechanisms.

To rule out potential artifacts, we performed the following set of control experiments: (1) the bare SWCNT FET devices were illuminated with alternating UV and visible light; (2) the tether (either dodecane or pyrene) without the spiropyran was introduced to the SWCNT FET. The devices are then exposed to UV/visible light with the same condition described above. The current–voltage curves are shown in the Supporting Information as Figures S6 and S7. There is no significant change in the FET characteristic, but only a slight change in the shape of the current–voltage curves when irradiated with UV and visible light. This minor difference is likely due to a myriad of background reactions in ambient conditions under irradiation.²

In addition, we have fabricated SWCNT FETs with the junctions between the carbon nanotube and the metal electrodes protected from the exposure to the self-assembled molecules. A Schottky barrier is known to form at these junctions and could, in principle, complicate the analysis.^{11,13} To eliminate this possibility, we covered the junctions with an insulating layer using hydrogensilsesquioxane resin (HSQ) that was patterned using electron beam lithography. These junction-protected devices were then immersed in solutions of **1a** and **2a**. The electrical properties are essentially the same as

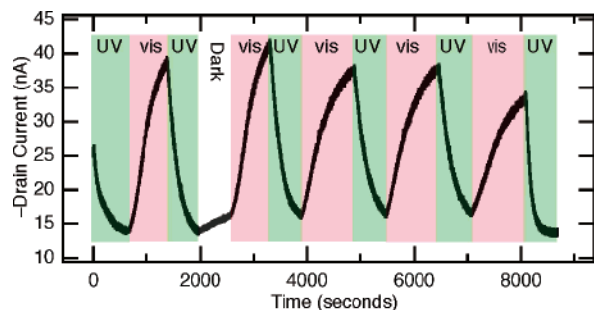


Figure 4. Time course of the drain current for a SWCNT transistor with **1a** assembled on its surface. The bias between the source and drain electrodes is 50 mV, and the gate bias is -9 V. Alternating irradiation with UV (365 nm) and visible light (633 nm). After ~ 2000 s, the device was measured in the dark and found to slowly revert back to the closed form of the spiropyran.

that shown in Figure 2 and Figure 3, indicating that the observed photoswitching effect of the molecules tethered on the SWCNT is responsible for the change in device characteristics. A micrograph of the device and current–voltage characteristics is in the Supporting Information (Figure S8).

Finally, we can gather kinetic data on this process for **1a** and **2a** by following the drain current as a function of time while the device is held at 50 mV source–drain bias and -9 V gate bias as the light is toggled between UV and visible wavelengths. A time trace for **1a** assembled on a SWCNT is shown in Figure 4. The device lifetime when switched in ambient atmosphere was ~ 10 switching cycles for these devices. The ring opening process (UV going from **1a** to **1b**) and cyclization (visible light going from **1b** to **1a**) can be fit to a single-exponential process. From the data in Figure 4, the forward and reverse rate constants, $k(\text{UV}) = 1.9 \pm 0.2 \times 10^{-3} \text{ s}^{-1}$ and $k(\text{visible}) = 1.5 \pm 0.1 \times 10^{-3} \text{ s}^{-1}$, were obtained. Other devices with **1a** had similar rate constants. The rate constants for **2a** were similar with $k(\text{UV}) = 1.4 \pm 0.2 \times 10^{-3} \text{ s}^{-1}$ and $k(\text{visible}) = 9.8 \pm 0.2 \times 10^{-4} \text{ s}^{-1}$. The time scale for this process is similar to that measured by Haddon and co-workers, the changes in the optical properties of mats of carbon nanotubes are covalently functionalized with spiropyran,⁷ but much faster than the rates of switching spiropyran in the crystalline state.¹⁴ This implies that the spiropyran is not tightly packed on the tube surface. The underlying photoprocess for the spiropyran is much faster¹⁵ than these values, and the slowness here is likely a reflection of the low probability for the chromophore to absorb a photon due to the low optical cross-section of the chromophore compared to the carbon nanotubes, the substrate, and the contacts. Moreover, we used only low-intensity, hand-held light sources for these experiments.⁸ As would be expected from studies on spiropyran in solution, there is also a slow dark process where the open form recycles to the closed spiropyran.⁶ After the third switching cycle shown in Figure 4, the device was left in the dark. To revert fully back to the high conductance state takes more than 6 h.

This study shows that photochromic molecules can be used to switch the conductance of a single-walled carbon nanotube transistor. In principle, the wavelengths to effect the forward and reverse photoprocesses could be varied through chemical synthesis, making a variety of devices that detect and respond to specific wavelengths of light. At a rudimentary level, these devices accomplish a task similar to biological processes, such as vision and photosynthesis, where light is sensed and converted into a signal. Here, we use a

combination of microfabrication and molecular self-assembly to produce field effect devices that detect the photoswitching events of around 10^4 molecules. This concept should naturally extend to biosensor applications either by sensing of conformational changes in tethered biomolecules or by biologically based recognition of one conformation of the spiropyran.¹⁶

Acknowledgment. We are grateful to Michael Steigerwald for enlightening discussions. We acknowledge primary financial support from the Academic Quality Fund at Columbia University and the Nanoscale Science and Engineering Initiative of the National Science Foundation under NSF Award Number CHE-0117752, and by the New York State Office of Science, Technology, and Academic Research (NYSTAR). C.N. thanks the American Chemical Society PRF type G (#39263-G7), the Camille Dreyfus Teacher Scholar Program (2004), and the Alfred P. Sloan Fellowship Program (2004). P.K. acknowledges support from an NSF CAREER award (DMR-0349232) and DARPA (N00014-04-1-0591).

Supporting Information Available: Synthetic details for the preparation of **1a** and **2a** and current–voltage curves for the control experiments mentioned in the text. This material is available free of charge via the Internet at <http://pubs.acs.org>.

References

- (1) (a) Tans, S. J.; Verschueren, A. R. M.; Dekker, C. *Nature* **1998**, *393*, 49–52. (b) Martel, R.; Schmidt, T.; Shea, H. R.; Hertel, T.; Avouris, P. *Appl. Phys. Lett.* **1998**, *73*, 2447–2449. (c) Avouris, P. *Acc. Chem. Res.* **2002**, *35*, 1026–1034.
- (2) Dai, H. *Acc. Chem. Res.* **2002**, *35*, 1035–1044.
- (3) (a) Chen, R. J.; Bangsaruntip, S.; Drouvalakis, K. A.; Kam, N. W. S.; Shim, M.; Li, Y.; Kim, W.; Utz, P. J.; Dai, H. *Proc. Natl. Acad. Sci. U.S.A.* **2003**, *100*, 4984–4989. (b) Someya, T.; Small, J.; Kim, P.; Nuckolls, C.; Yardley, J. T. *Nano Lett.* **2003**, *3*, 877–881. (c) Star, A.; Han, T.-R.; Gabriel, J.-C. P.; Bradley, K.; Gruener, G. *Nano Lett.* **2003**, *3*, 1421–1423. (d) Star, A.; Gabriel, J.-C. P.; Bradley, K.; Gruener, G. *Nano Lett.* **2003**, *3*, 459–463. (e) Star, A.; Han, T.-R.; Joshi, V.; Gabriel, J.-C. P.; Gruener, G. *Adv. Mater.* **2004**, *16*, 2049–2052. (f) Bradley, K.; Briman, M.; Star, A.; Gruener, G. *Nano Lett.* **2004**, *4*, 253–256. (g) Star, A.; Joshi, V.; Han, T.-R.; Altoe, M. V. P.; Gruener, G.; Stoddart, J. F. *Org. Lett.* **2004**, *6*, 2089–2092.
- (4) (a) Misewich, J. A.; Avouris, P.; Martel, R.; Tsang, J. C.; Heinze, S.; Tersoff, J. *Science* **2003**, *300*, 783–786. (b) Chen, R. J.; Franklin, N. R.; Kong, J.; Cao, J.; Tomblor, T. W.; Zhang, Y.; Dai, H. *Appl. Phys. Lett.* **2001**, *79*, 2258–2260. (c) Star, A.; Lu, Y.; Bradley, K.; Gruener, G. *Nano Lett.* **2004**, *4*, 1587–1591.
- (5) (a) Bertelson, R. C. In *Organic Photochromic and Thermochemical Compounds*; Crano, J. C., Guglielmetti, R. J., Eds.; Springer: Berlin, 1999; pp 11–83. (b) Shipway, A. N.; Katz, E.; Willner, I. *Struct. Bonding* **2001**, *99*, 237–281. (c) Guglielmetti, R. *Photochromism*; Elsevier: Amsterdam, 2003; pp 855–878.
- (6) Berkovic, G.; Krongauz, V.; Weiss, V. *Chem. Rev.* **2000**, *100*, 1741–1753.
- (7) Khairutdinov, R. F.; Itkis, M. E.; Haddon, R. C. *Nano Lett.* **2004**, *4*, 1529–1533.
- (8) Details are contained in the Supporting Information.
- (9) Syntheses of **1** and **2** followed those of: Guo, X.; Zhang, D.; Zhou, Y.; Zhu, D. *J. Org. Chem.* **2003**, *68*, 5681–5687.
- (10) (a) Huang, L.; Cui, X.; White, B.; O'Brien, S. P. *J. Phys. Chem. B* **2004**, *108*, 16451–16456. (b) Huang, L.; Wind, S. J.; O'Brien, S. P. *Nano Lett.* **2003**, *3*, 299–303.
- (11) Appenzeller, J.; Knoch, J.; Radosavljevic, M.; Avouris, P. *Phys. Rev. Lett.* **2004**, *92*, 226802/226801–226802/226804.
- (12) Klinke, C.; Chen, J.; Afzali, A.; Avouris, P. *Nano Lett.* **2005**, *5*, 555–558.
- (13) (a) Chen, R. J.; Choi, H. C.; Bangsaruntip, S.; Yenilmez, E.; Tang, X.; Wang, Q.; Chang, Y.-L.; Dai, H. *J. Am. Chem. Soc.* **2004**, *126*, 1563–1568. (b) Someya, T.; Kim, P.; Nuckolls, C. *Appl. Phys. Lett.* **2003**, *82*, 2338–2340.
- (14) Benard, S.; Yu, P. *Adv. Mater.* **2000**, *12*, 48–50.
- (15) Tamai, N.; Miyasaka, H. *Chem. Rev.* **2000**, *100*, 1875–1890.
- (16) Blonder, R.; Ben-Dov, I.; Dagan, A.; Willner, I.; Zisman, E. *Biosens. Bioelectron.* **1997**, *12*, 627–644.

JA054335Y